[REVISI HASIL PENILAIAN SEBELUMNYA]

DOKUMEN INI BERISI:

1. **KATA PENGANTAR**
2. **PAPER DARI 4 NEGARA**
3. **PAPER SENDIRI**

1. HALAMAN AWAL DAN KATA PENGANTAR

Pembicara dari 4 negara: Indonesia, Japan, Singapore, Malaysia

LINK: https://pubs.aip.org/aip/acp/article/2543/1/010001/2828968/Preface-The-4th-EPI-International-Conference-on

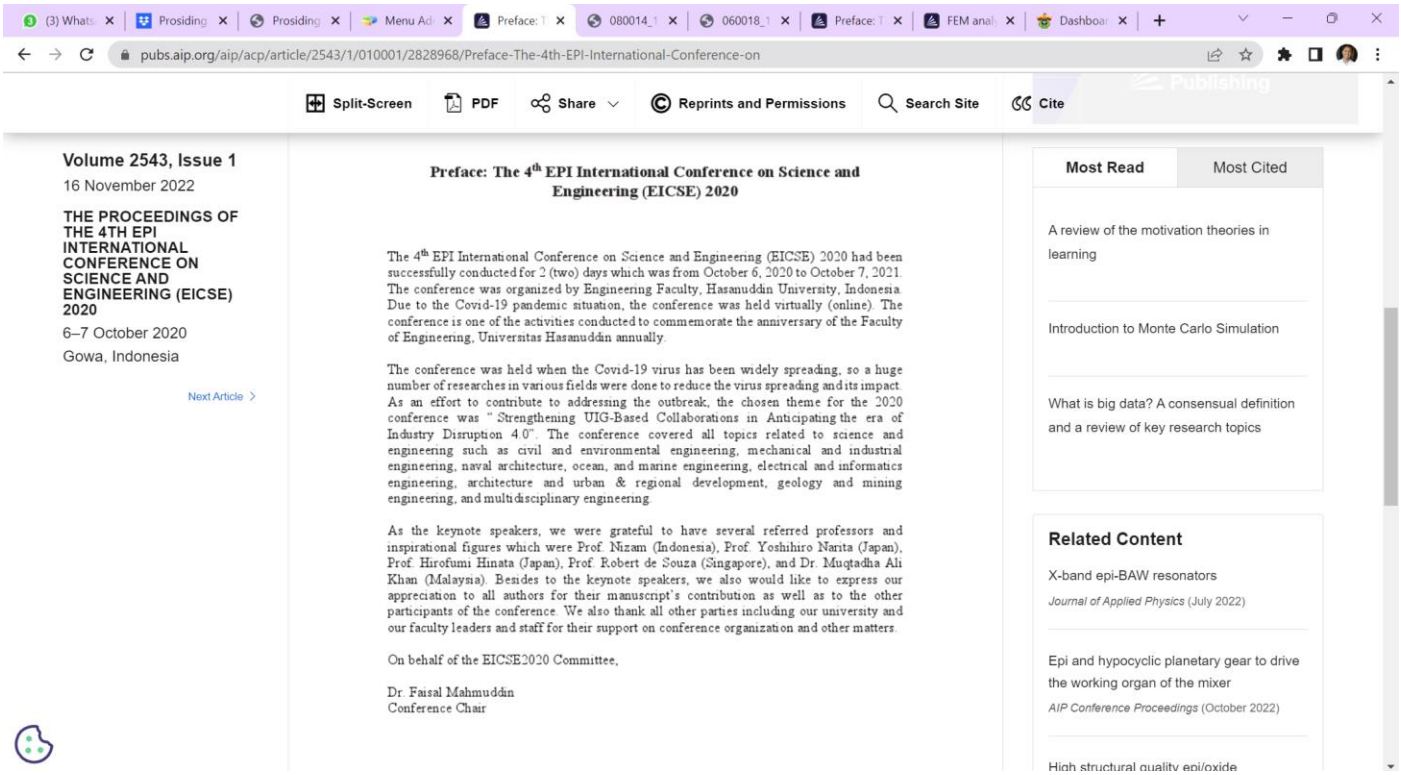

Split-Screen PDF Share Reprints and Permissions Search Site Cite

Volume 2543, Issue 1
16 November 2022

THE PROCEEDINGS OF THE 4TH EPI INTERNATIONAL CONFERENCE ON SCIENCE AND ENGINEERING (EICSE) 2020
6–7 October 2020
Gowa, Indonesia

Next Article >

Preface: The 4th EPI International Conference on Science and Engineering (EICSE) 2020

The 4th EPI International Conference on Science and Engineering (EICSE) 2020 had been successfully conducted for 2 (two) days which was from October 6, 2020 to October 7, 2021. The conference was organized by Engineering Faculty, Hasanuddin University, Indonesia. Due to the Covid-19 pandemic situation, the conference was held virtually (online). The conference is one of the activities conducted to commemorate the anniversary of the Faculty of Engineering, Universitas Hasanuddin annually.

The conference was held when the Covid-19 virus has been widely spreading, so a huge number of researches in various fields were done to reduce the virus spreading and its impact. As an effort to contribute to addressing the outbreak, the chosen theme for the 2020 conference was " Strengthening UIG-Based Collaborations in Anticipating the era of Industry Disruption 4.0". The conference covered all topics related to science and engineering such as civil and environmental engineering, mechanical and industrial engineering, naval architecture, ocean, and marine engineering, electrical and informatics engineering, architecture and urban & regional development, geology and mining engineering, and multidisciplinary engineering.

As the keynote speakers, we were grateful to have several referred professors and inspirational figures which were Prof. Nizam (Indonesia), Prof. Yoshihiro Narita (Japan), Prof. Hirofumi Hinata (Japan), Prof. Robert de Souza (Singapore), and Dr. Muqtadha Ali Khan (Malaysia). Besides to the keynote speakers, we also would like to express our appreciation to all authors for their manuscript's contribution as well as to the other participants of the conference. We also thank all other parties including our university and our faculty leaders and staff for their support on conference organization and other matters.

On behalf of the EICSE2020 Committee,

Dr. Faisal Mahmuddin
Conference Chair

Most Read | Most Cited

A review of the motivation theories in learning

Introduction to Monte Carlo Simulation

What is big data? A consensual definition and a review of key research topics

Related Content

X-band epi-BAW resonators
Journal of Applied Physics (July 2022)

Epi and hypocyclic planetary gear to drive the working organ of the mixer
AIP Conference Proceedings (October 2022)

High structural quality epi/oxide

2. PAPER DARI PESERTA MINIMAL 4 NEGARA

JAPAN

LINK: https://pubs.aip.org/aip/acp/article/2543/1/060018/2829271/FEM-analysis-for-in-plane-vibration-of-rectangular

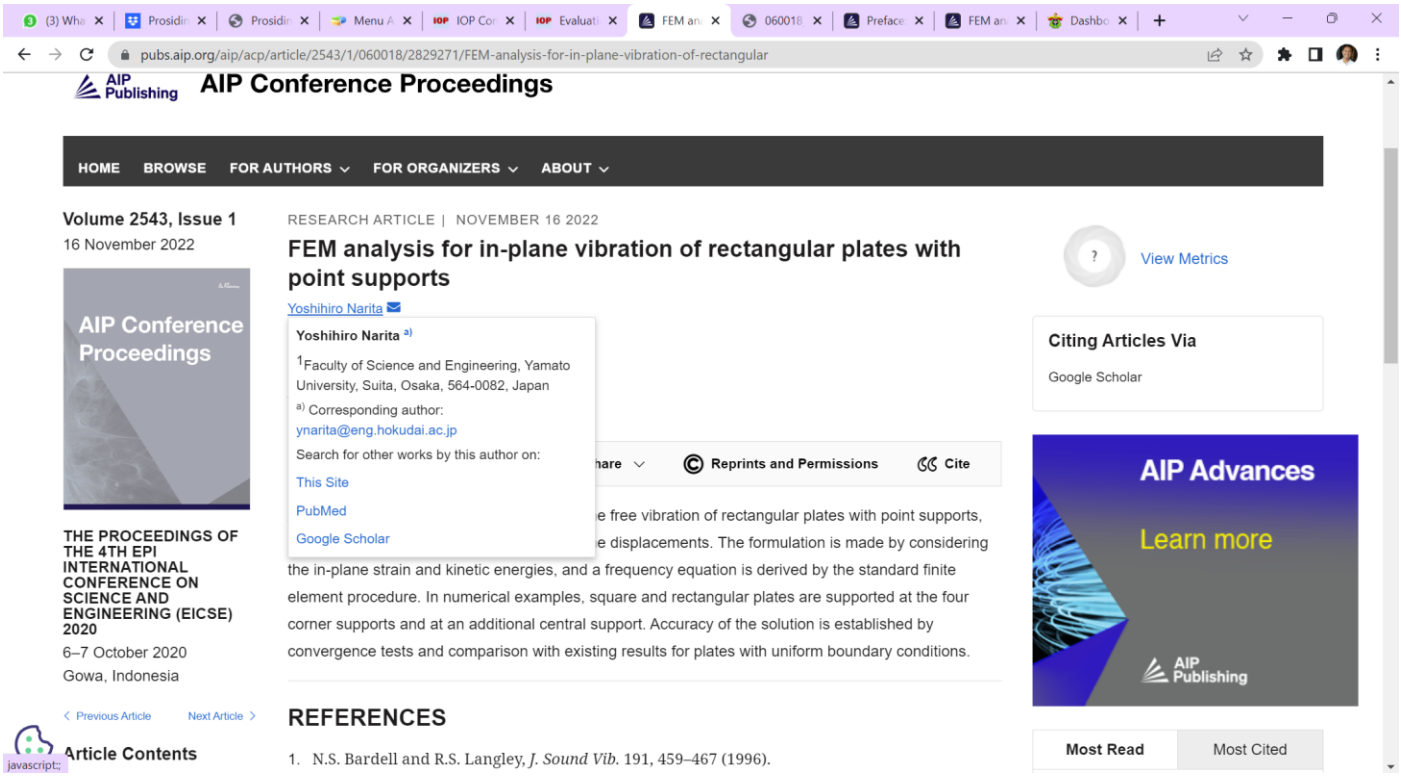

AIP Publishing AIP Conference Proceedings

HOME BROWSE FOR AUTHORS FOR ORGANIZERS ABOUT

Volume 2543, Issue 1
16 November 2022

THE PROCEEDINGS OF THE 4TH EPI INTERNATIONAL CONFERENCE ON SCIENCE AND ENGINEERING (EICSE) 2020
6–7 October 2020
Gowa, Indonesia

< Previous Article Next Article >

Article Contents

RESEARCH ARTICLE | NOVEMBER 16 2022

FEM analysis for in-plane vibration of rectangular plates with point supports

Yoshihiro Narita

Yoshihiro Narita [a)]
[1]Faculty of Science and Engineering, Yamato University, Suita, Osaka, 564-0082, Japan
[a)] Corresponding author: ynarita@eng.hokudai.ac.jp
Search for other works by this author on:
This Site
PubMed
Google Scholar

Reprints and Permissions Cite

e free vibration of rectangular plates with point supports, e displacements. The formulation is made by considering the in-plane strain and kinetic energies, and a frequency equation is derived by the standard finite element procedure. In numerical examples, square and rectangular plates are supported at the four corner supports and at an additional central support. Accuracy of the solution is established by convergence tests and comparison with existing results for plates with uniform boundary conditions.

REFERENCES

1. N.S. Bardell and R.S. Langley, *J. Sound Vib.* 191, 459–467 (1996).

View Metrics

Citing Articles Via
Google Scholar

Most Read | Most Cited

MALAYSIA

LINK: https://pubs.aip.org/aip/acp/article/2543/1/080014/2829362/Computational-investigation-into-resistance

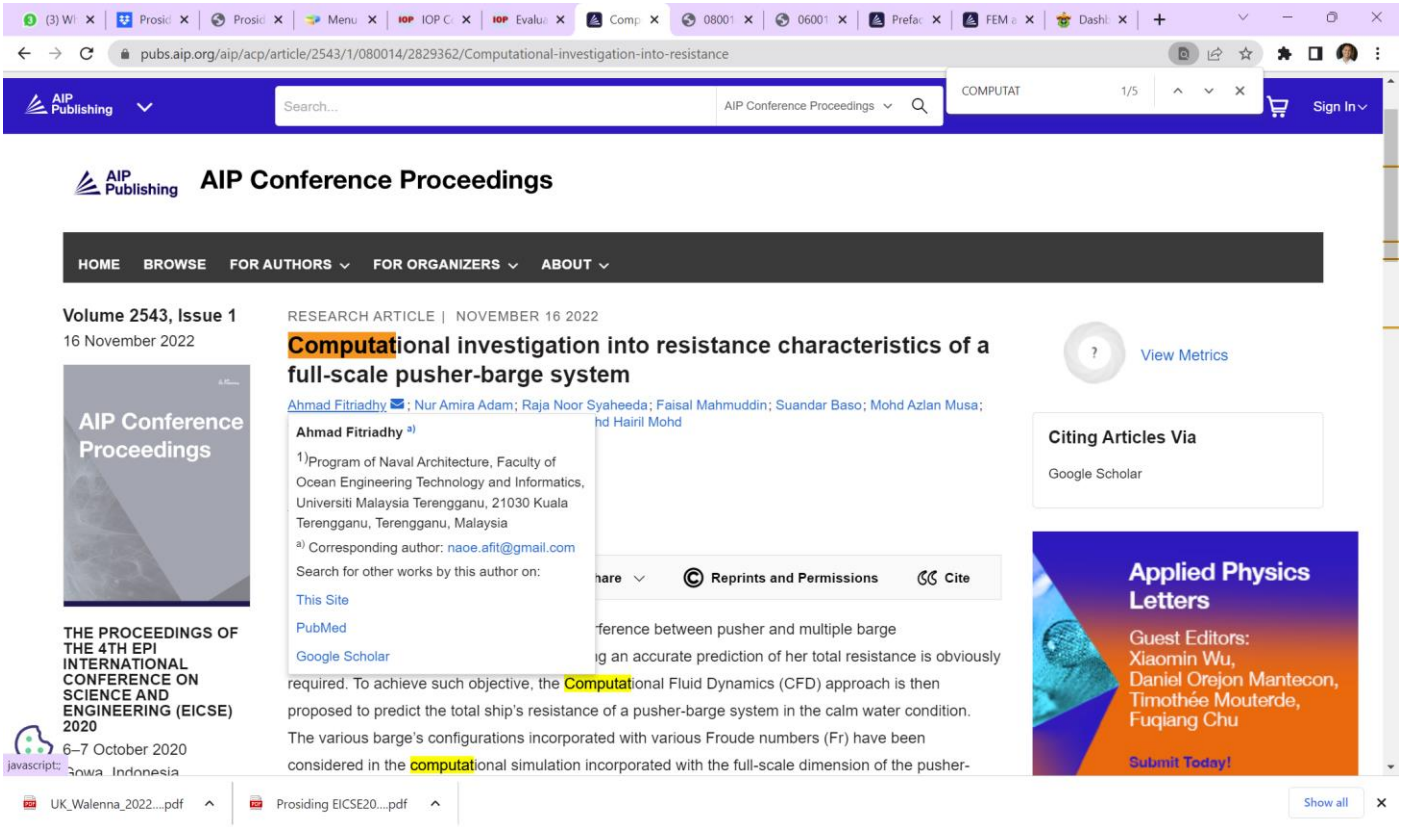

TOGO

LINK: https://pubs.aip.org/aip/acp/article/2543/1/070002/2829379/New-approximate-analytical-solutions-for-time-step

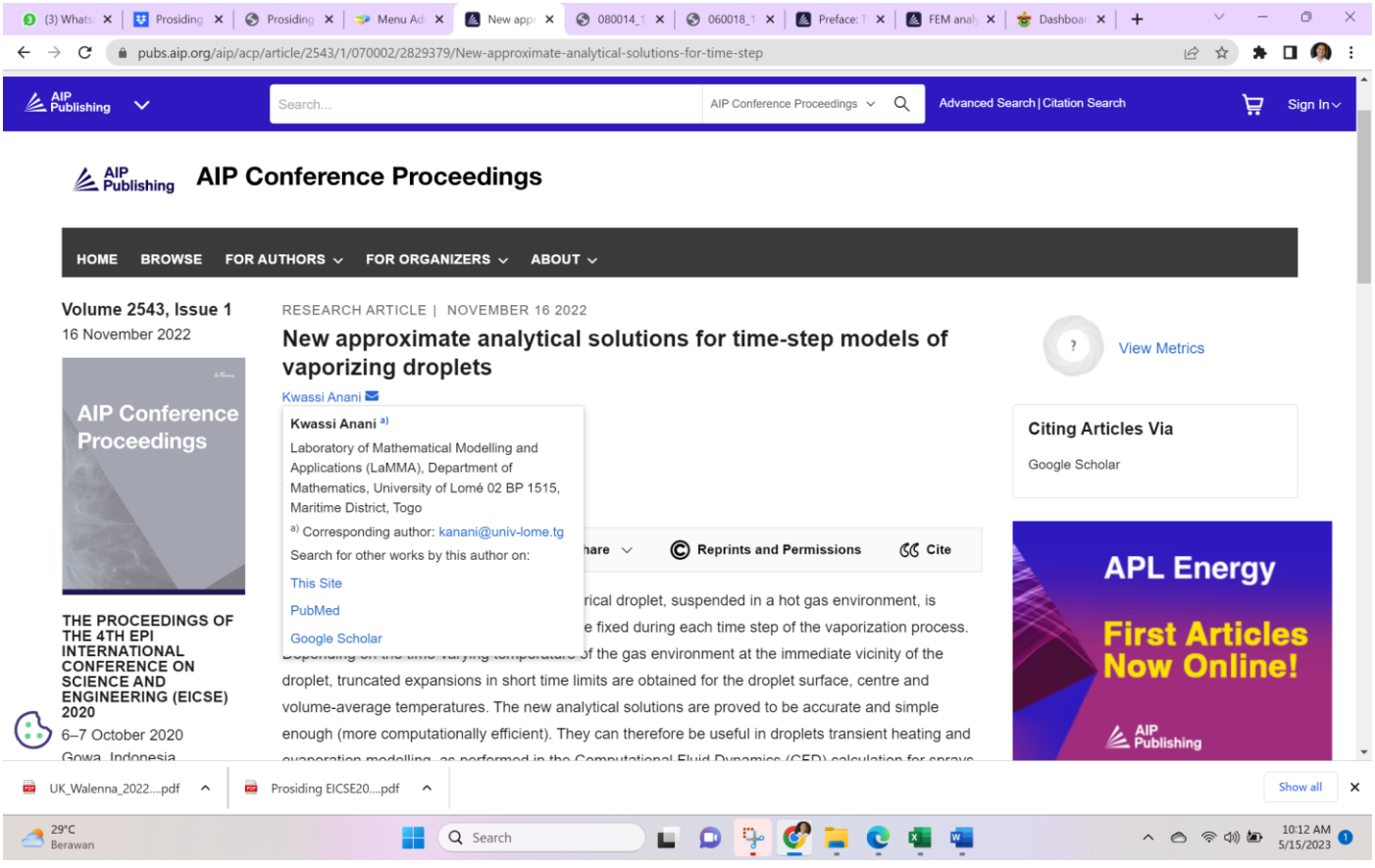

INDONESIA (PAPER SENDIRI)

LINK: https://pubs.aip.org/aip/acp/article/2543/1/030013/2829258/FEM-analysis-of-hybrid-composite-beams-made-of

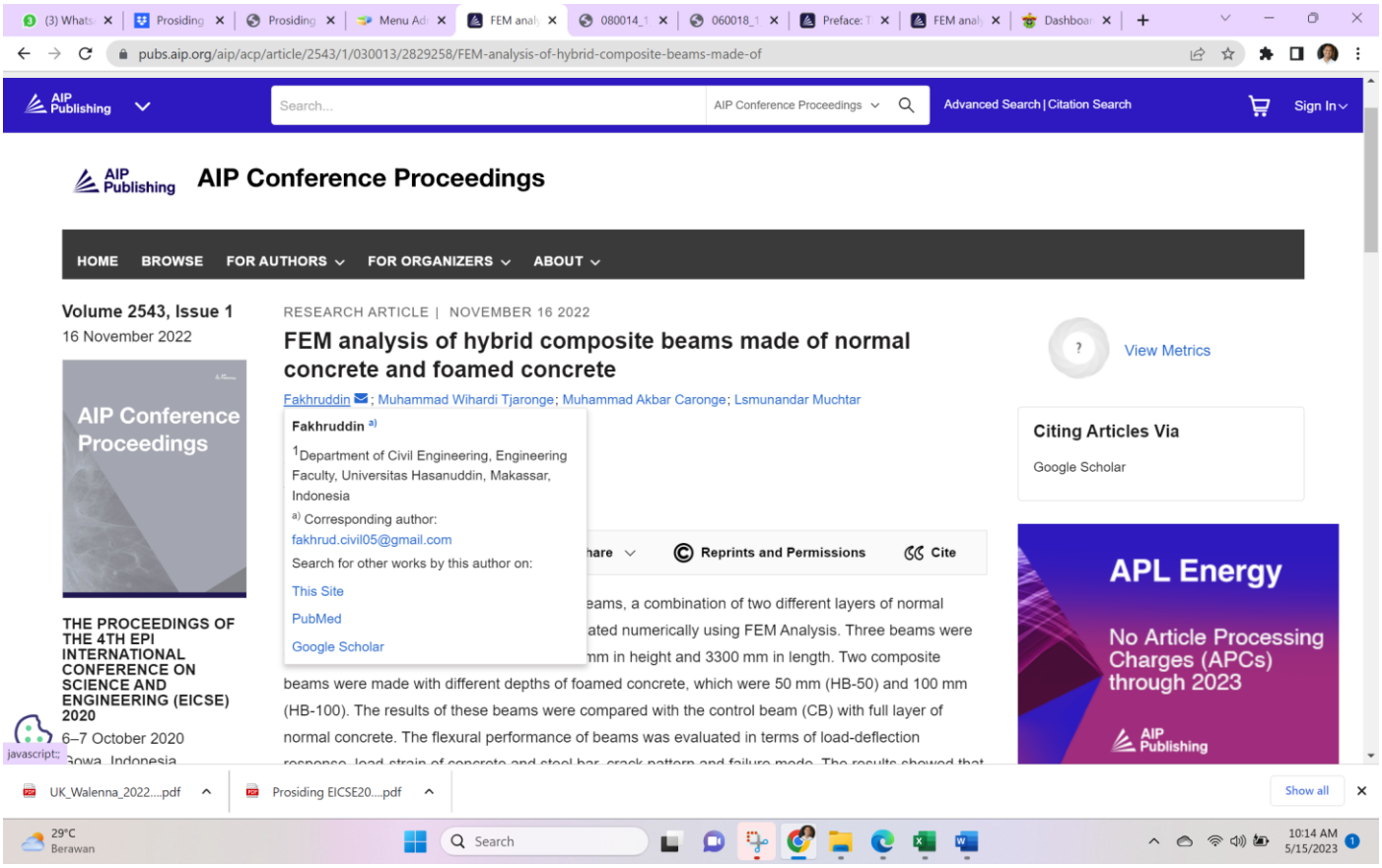

FEM analysis of hybrid composite beams made of normal concrete and foamed concrete

Cite as: AIP Conference Proceedings **2543**, 030013 (2022); https://doi.org/10.1063/5.0094742
Published Online: 16 November 2022

Fakhruddin, Muhammad Wihardi Tjaronge, Muhammad Akbar Caronge, et al.

FEM Analysis of Hybrid Composite Beams Made of Normal Concrete and Foamed Concrete

Fakhruddin[1,a)], Muhammad Wihardi Tjaronge[1,b)], Muhammad Akbar Caronge[1,c)], and Ismunandar Muchtar[1,d)]

[1]*Department of Civil Engineering, Engineering Faculty, Universitas Hasanuddin, Makassar, Indonesia*

[a)]Corresponding author: fakhrud.civil05@gmail.com
[b)]tjaronge@yahoo.co.id
[c)]caronge.eng@yahoo.co.id
[d)]ismunandar@gmail.com

Abstract. Flexural performances of hybrid composite beams, a combination of two different layers of normal concrete and foamed concrete, were investigated numerically using FEM Analysis. Three beams were tested with dimension 150 mm in width, 200 mm in height and 3300 mm in length. Two composite beams were made with different depths of foamed concrete, which were 50 mm (HB-50) and 100 mm (HB-100). The results of these beams were compared with the control beam (CB) with full layer of normal concrete. The flexural performance of beams was evaluated in terms of load-deflection response, load-strain of concrete and steel bar, crack pattern and failure mode. The results showed that foamed concrete at hybrid composite beams reduced the ultimate load of the beams. Compared to the control beam, the ultimate load of HB-50 and HB-100 was decreased by 29.5% and 30.8%, respectively. However, different depth of foamed concrete at the hybrid beams showed an insignificant effect on the ultimate load. The number of cracks on HB-50 and HB-100 was larger than that of CB. Some cracks in foam concrete do not propagate upward to the normal concrete layer. Finally, all the beams failed under the crushing of compression concrete.

INTRODUCTION

Today, the number at which concrete is used is much higher than 40 years ago [1]. The estimation of the present consumption of concrete in the world is 11 billion metric tonnes every year. Concrete has many advantages over other materials such as possesses excellent resistance to water, can be formed into a variety of shapes and sizes and the cheapest and most readily available material on the job [1]. The principal components for making concrete, namely aggregate, water, and portland cement are relatively inexpensive and are commonly available in most parts of the world.

Massive exploration of the natural materials for producing concretes affects the environmental condition and global warming that may cause disasters such as flooding and landslides. Therefore, it is necessary to reduce the effect of concrete materials on the environmental impact. The concrete should be used as efficiently as possible. Thus, the research on the fields of concrete efficiency should be conducted intensively.

The natural behavior of concrete material is strong in compression and weak in tension. The tensile strength of concrete is about 8 to 15 percent of the compression strength [2,3,4]. Therefore the contribution of the tensile strength of concrete to the flexural capacity of the beams is neglected as illustrated in Fig. 1. The flexural capacity of the beam is influenced only by the compression stress of the concrete and the tensile stress of the steel reinforcement [2], as expressed in Eqs. (1) and (2).

The Proceedings of the 4th EPI International Conference on Science and Engineering (EICSE) 2020
AIP Conf. Proc. 2543, 030013-1–030013-11; https://doi.org/10.1063/5.0094742
Published by AIP Publishing. 978-0-7354-4358-7/$30.00

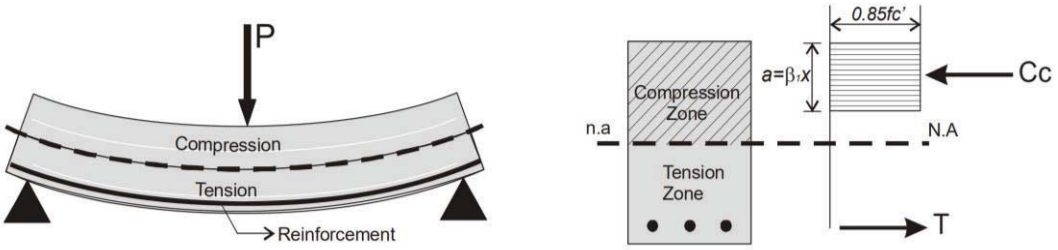

FIGURE 1. Compression and tension zone of RC beam due to flexure [4]

$$M_n = 0.85 f_c' \beta_1 b \left(d - \frac{1}{2}a\right) \quad (1)$$

$$M_n = A_s f_y \left(d - \frac{1}{2}a\right) \quad (2)$$

where f'_c is the concrete strength, b is width of the beam, d is the effective depth of the beam, a is depth of equivalent rectangular stress block, A_s is area of steel rebars, and f_y is yield stress of steel bars.

In order to efficiently use the concrete materials, then the compressive strength of the concrete on the tensile stressed section may be reduced, or the concrete on the tensile stressed section may be removed. However, this will affect to the durability of the concrete structure. Some methods have been studied to replace concrete on the tensile stressed section such as the use of hollow concrete [5,6,7], engineered cementitious composites [8] and styrofoam concrete [9].

This study developed foamed concrete to replace concrete on the tensile stressed section. Research about the mechanical properties of foamed concrete has been investigated by many researchers [10,11,12,13,14,15,16]. Foamed concrete or cellular concrete is either a mortar or cement pastes in which air voids are artificially entrapped in mortar. Foamed concrete has advantages such as low self-weight, high flowability, minimal usage of aggregate, controlled low strength, and excellent thermal insulation properties. Due to its lightweight and more economical nature, its applications as a lightweight material in the construction industry are gaining growing popularity. Foamed concrete has low compressive strength, therefore, its application on the hybrid structure may affect the behaviour of structures.

In this regard, this study investigates the effect of foamed concrete on the flexural behaviour of hybrid composite beams made of normal concrete and foamed concrete. This study was conducted numerically by using FEM Analysis software. The flexural performance of beams was evaluated in terms of load-deflection response, load-strain of concrete and steel bar, crack pattern and failure mode.

FOAMED CONCRETE

Foamed concrete is a mortar or cement pastes in which air voids are artificially entrapped in mortar. It possesses low self-weight, high flowability, minimal usage of aggregate, controlled low strength, and excellent thermal insulation properties. Foam concretes are given their structure for foaming by using foam generators or stirring up the cement paste using foaming agents and fast rotating pug mill mixers. The paste consists of the binder, usually cement, finely grounded quartzitic sand, water and foam generating admixtures. After molding the foam, the concrete hardens under normal atmospheric conditions [10].

The foamed concrete consisted of Portland cement, sand, foam agent and admixture as shown in Fig. 2. The mix design of foamed concrete was presented in Table 1. The type of foam agent was Texapon N70. It is a highly concentrated sodium lauryl ether sulphate derived from natural fatty alcohols. During the mechanical foaming procedure, a foam agent is added to the mortar. Numerous bubbles are mechanically introduced by high-speed mixers. A relatively unstable foam develops with an irregular structure and undefined void structures [17]. In practice, a more usual manufacturing method is physical foaming. A pre-manufactured foam consisting of water and the chemical admixture is mixed with the additional components. Under these conditions, a more stable and fine-pored mortar will result [17].

FIGURE 2. Materials in foamed concrete

TABLE 1. Mix design of foamed concrete (per m^3)

Cement	Sand	Water	Sikament LN	Foam Agent
662.5 kg	1,325 kg	232 liter	16.6 kg	30% of mortar portion

FEM MODELLING

Geometry and Meshing

The geometric details of the numerical models were defined according to the specimen as shown in Fig. 3. A total of three beams were investigated by using FEM analysis. Detail of all beams is shown in Table 2. The dimension of beams was 150 mm in width, 200 mm in height and 3300 mm in length. Two composite beams were made with depth of foamed concrete was 50 mm and 100 mm. The results of these beams were compared with the control beam made of full layer of normal concrete.

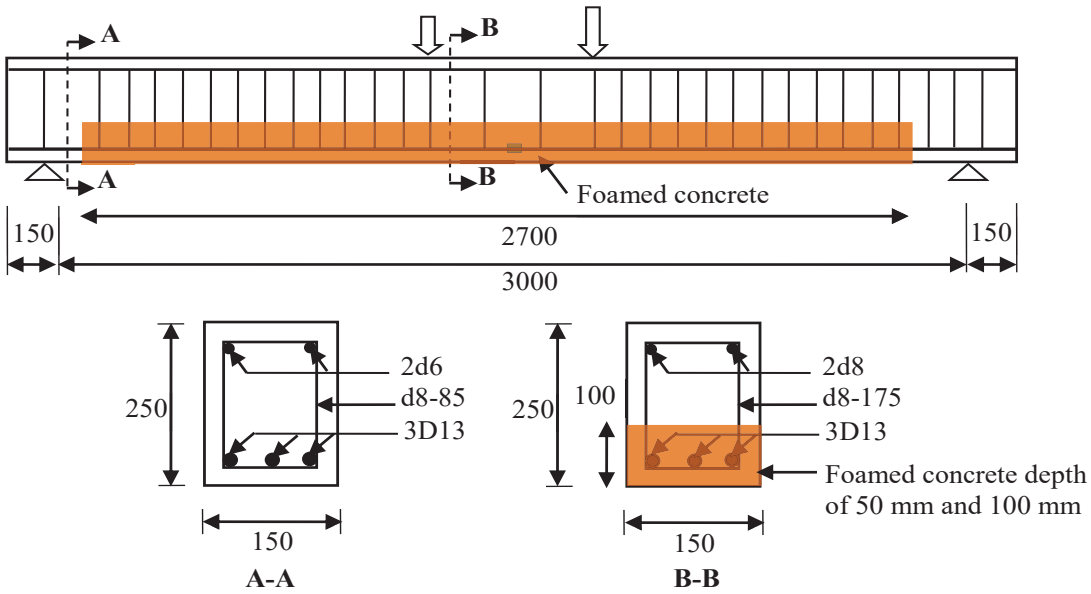

FIGURE 3. The geometric detail of specimens

TABLE 2. Variation of specimens

Beam code	Depth of foamed concrete (mm)	Remark
CB	-	Control beam
HB-50	50	Hybrid beam
HB-1100	100	Hybrid beam

A nonlinear plane stress analysis is to be carried out on a model of a reinforced concrete beam. The 2-dimensional model of control beam and hybrid beam is shown in Figs. 4 and 5, respectively. The reinforcement was provided in the lower and upper face of the beam has a total cross-section area of 397.9 mm^2 (3D13) and 100.5 mm^2 (2d8), respectively. The reinforcement was also provided at the vertical direction of the beam as the transverse rebars with the total cross-section of 100.5 mm^2. The superposition of nodal degrees of freedom assumes that the concrete and reinforcement were perfectly bonded. It was assumed that the self-weight of the beam is negligible compared with the applied load.

The model of control beam consists of two parts: the concrete elements and the steel elements (reinforcement and dowels). The model of hybrid composite beam consists of four parts: the normal concrete element, the foam concrete element, the steel elements (reinforcement and dowels) and interface between normal concrete and foamed concrete. The concrete beam was modeled as surface while the reinforcement was defined as a line. The reinforcement was modeled by the bar element during analysis. The mesh division of a 50 mm square was adopted for the analysis

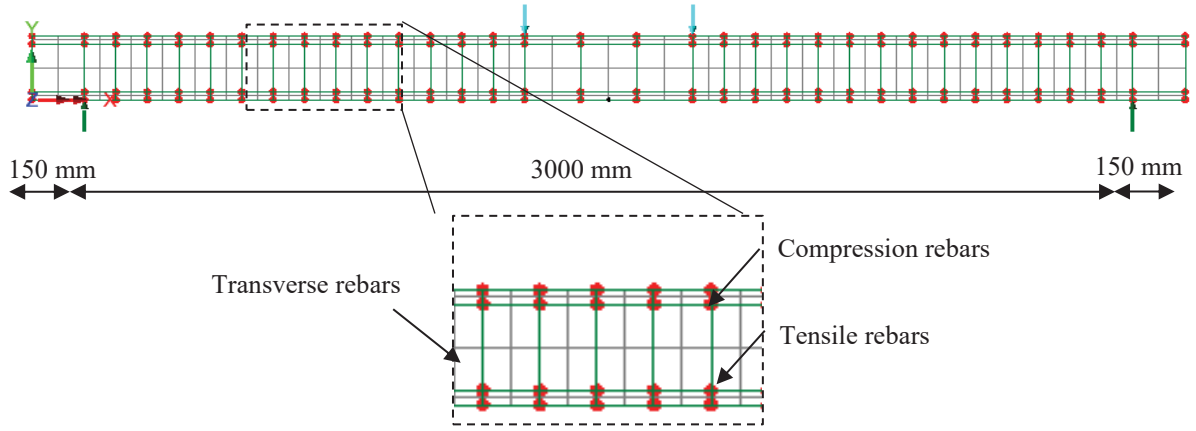

FIGURE 4. Numerical model of control beam (NC)

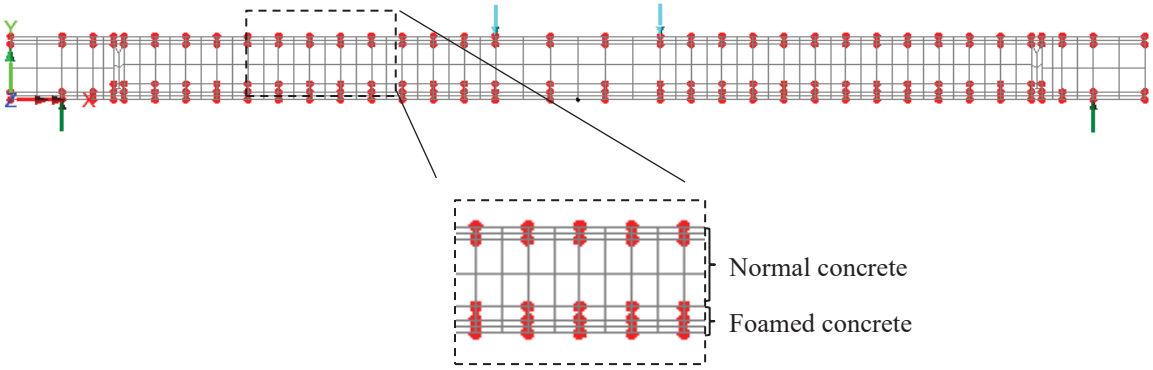

FIGURE 5. Numerical model of hybrid beam

Material Properties and Model

Concrete

To define the mechanical properties of normal concrete and foamed concrete, uniaxial compression tests were performed on cylinder specimens with dimension of 100x200 mm. Compressive and tensile strength test were conducted by using Universal Testing Machine at the age of 28 days as shown in Fig. 6. The compressive and tensile strength tests followed ASTM C39 [18] and ASTM C78 [19] specifications, respectively. Properties of normal concrete and foamed concrete were presented in Table 3.

a. Compressive strength test b. Tensile strength test

FIGURE 6. Compressive and tensile strength test

TABLE 3. Properties of normal concrete and foamed concrete

	Normal concrete	Foamed concrete
Compressive strength (MPa)	20.37	5.70
Tensile strength (MPa)	2.07	0.52
Modulus of Elasticity (MPa)	21209	3823

In FEM Analysis, the typical stress-strain of the concrete that was used is shown in Fig. 7. A multi-crack concrete (Model 94) was used. The multi-crack concrete model is a plastic-damage-contact model in which damage planes form according to a principal stress criterion and then develop as embedded rough contact planes. In this model, the input data was uniaxial compressive strength (f_c), uniaxial tensile strain (f_t), strain at peak uniaxial compression (ε_c), strain at effective end of softening curve for distributed fracture (ε_0), fracture energy per unit area (G_f).

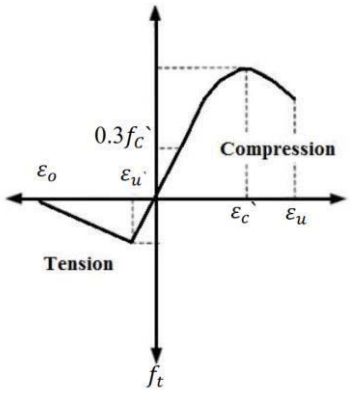

FIGURE 7. Stress-strain curve of concrete

Reinforcement

The properties of steel bars were determined by conducting a tensile strength test in the laboratory as shown in Fig. 8. The yielding stress (f_y), yielding strain (ε_y) and Young modulus (E) of steel bars were presented in Table 4.

TABLE 4. Properties of steel bars

Steel bars diameter (mm)	Yield stress (MPa)	Yield strain ($\mu\varepsilon$)	Young Modulus (MPa)
8	377.87	1960	193038
13	388.32	2020	214543

FIGURE 8. Tensile strength of rebars

In FEM analysis, the steel bars are modeled by means of the embedded reinforcement element (perfect bounding). A bilinear elasto-plastic constitutive model is used to appropriately represent the stress-strain relationship of reinforcing bars as shown in Fig. 9.

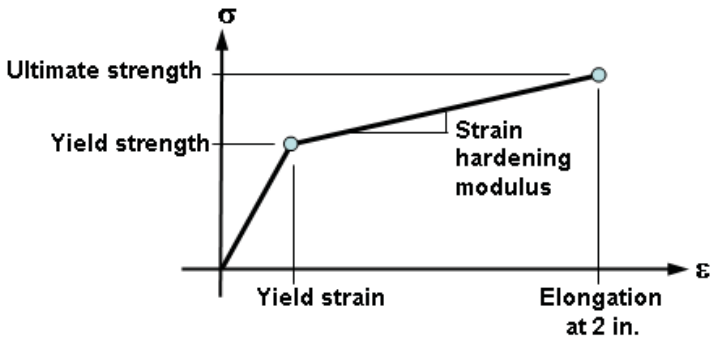

FIGURE 9. Stress-strain of steel bars

Boundary Condition and Loading Point

A simply supported boundary condition was assigned at the bottom of the beam at 150 mm from the edge. Two-point loads were applied to the top of the beams at a distance of 1450 mm from the edge. This was to simulate a four-point bending test as shown in Fig. 10. Plane stress (QPM8) elements represented the concrete section, and bar (BAR3) elements presented the reinforcement bars.

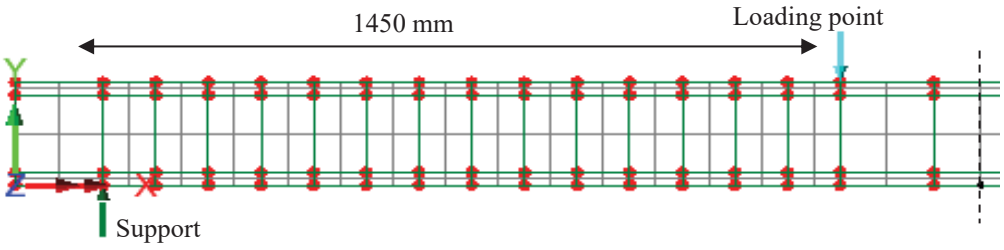

FIGURE 10. The boundary of beam at FEM analysis

RESULTS AND DISCUSSION

Load-Deflection Curves

Figure 11 shows the load and deflection responses of all beams and the results of FEM Analysis are summarized in Table 5. The deflection reported here was the deflection at the mid-span of the beam. Generally, all the beams exhibited similar behavior until the first crack. After that, the slope of load-deflection curves reduced gradually. The slope of CB was higher than that of HB-50 and HB-100. Meanwhile, the stiffness of HB-50 and HB-100 was almost similar. This indicates that the use of foamed concrete at the hybrid beams affected the stiffness of the beams. However, the different depth of foamed concrete at the hybrid beam did not significantly affect the stiffness.

After the yielding load, the slope of load and deflection curve reduced significantly. The load was constant, while the displacement still increased until the failure. This was a typical flexural failure mode.

As shown in Table 5, the first cracking load and deflection of CB were 5 kN and 0.53 mm, respectively. The first cracking load and deflection of HB-50 were 5 kN and 1.60 mm, respectively. The first cracking load and deflection of HB-100 were 4 kN and 1.55 mm, respectively. This indicated that the first cracking load almost similar in all beams but the deflection of hybrid beam was higher than that of normal beam.

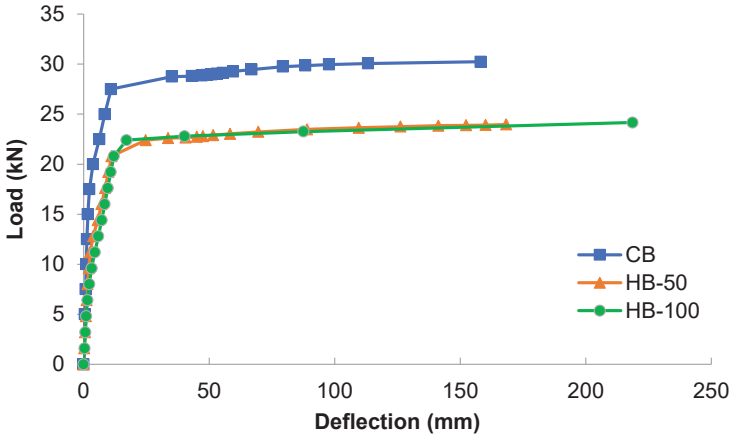

FIGURE 11. Load-deflection responses

TABLE 5. Results of FEM analysis

Beam	First crack		Yield		Ultimate		Failure mode
	P_{cr} (kN)	Δ_{cr} (mm)	P_y (kN)	Δ_y (mm)	P_u (kN)	Δ_u (mm)	
CB	5	0.53	27.5	10.91	30.2	158.19	Flexural failure
HB-50	5	1.60	18.2	11.16	21.3	180.44	Flexural failure
HB-100	4	1.55	18.2	12.01	20.9	218.64	Flexural failure

At yielding, the load and deflection of CB was 27.5 kN and 10.91 mm, respectively. HB-50 was 18.2 kN and 11.16 mm, respectively and HB-100 was 17.8 kN and 12.01 mm, respectively. Compared to CB, the yielding load of HB-50 and HB-100 was decreased by 33.8% and 35.3%, respectively. It means that the use of foamed concrete at hybrid composite beam reduced the yielding load of the beams. However, the different depth of foamed concrete at the hybrid beam showed an insignificant effect on the yielding load.

Finally, at the failure, the ultimate load and deflection of CB was 30.2 kN and 158.19 mm, respectively. HB-50 was 24.0 kN and 180.44 mm, respectively and HB-100 was 23.8 kN and 218.64 mm, respectively. Compared to CB, the ultimate load of HB-50 and HB-100 was decreased by 29.5% and 30.8%, respectively. This indicated that the use of foamed concrete at hybrid composite beams reduced the ultimate load of the beams. Similar to yielding load, the different depth of foamed concrete at the hybrid beams also showed an insignificant effect on the ultimate load

Load-Strain Curves

Figures 12a and b show the load and strain curves of steel bars and concrete, respectively. The location of steel gauge was at the middle of the longitudinal rebars, while the location of the concrete gauge was at upper surface of the beam.

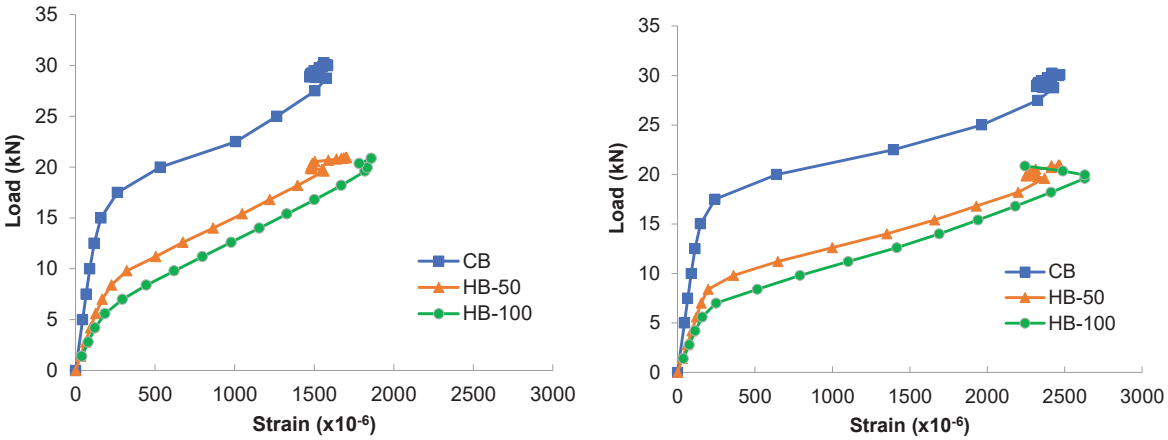

a. Longitudinal rebars

b. Concrete

FIGURE 12. Load-strain curves

As shown, the longitudinal rebars has reached the yielding strain of 1500 $\mu\varepsilon$ and the concrete also has reached the ultimate strain of 2500 $\mu\varepsilon$. The longitudinal rebars were yielded before the failure of concrete at the compression zone. This was a typical under-reinforced failure mode. Therefore, the use of foamed concrete at the hybrid beams did not change the failure mode of the beam which was failed under crushing of compression concrete.

Crack Pattern

Figure 13 showed the crack pattern of all beams at the first crack. The first crack of CB, HB-50 and GHB-100 was 5 kN, 5 kN and 4 kN, respectively. This crack occurred at the constant moment region. Further loading after the appearance of the first crack, the other cracks appeared while the existing cracks propagated. The propagation of the cracks moved toward the compression concrete. The long cracks were concentrated in the constant moment region at the span center.

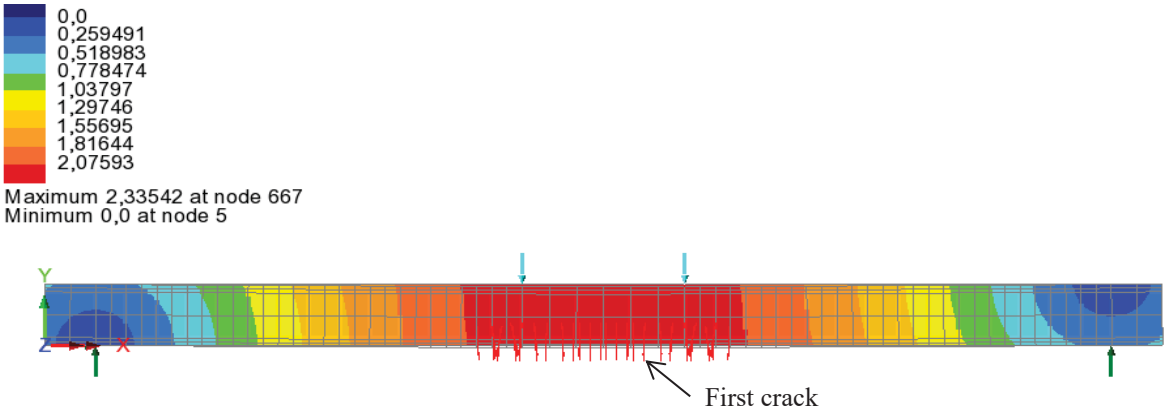

a. CB

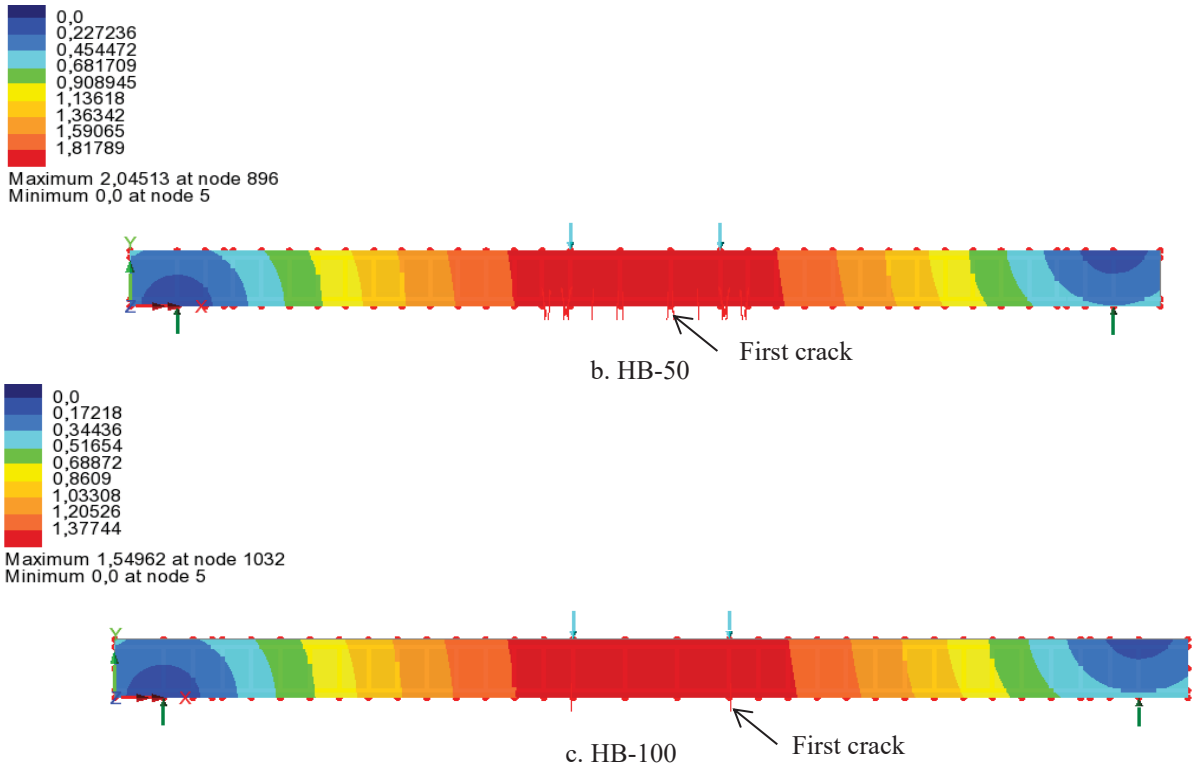

FIGURE 13. Crack pattern at the first crack

Figure 14 shows the crack pattern of all beams at the ultimate load. The ultimate load of CB, HB-150 and HB-100 was 30.2 kN, 21.3 kN and 20.9 kN, respectively. Comparing to cracks number of the normal beams, the number of cracks on HB-50 and HB-100 was larger. The long cracks were concentrated in the constant moment region at the span center. The number of cracks on the tensile zone of the concrete on HB-50 and HB-100 was larger than that of CB. This was because the foam concrete has a low tensile strength compared to normal concrete. Also, the cracks that occur in the foam concrete do not propagate upward to the normal concrete layer. This was because there are interfaces in the foam concrete and normal concrete, thereby reducing the composite action of the beam.

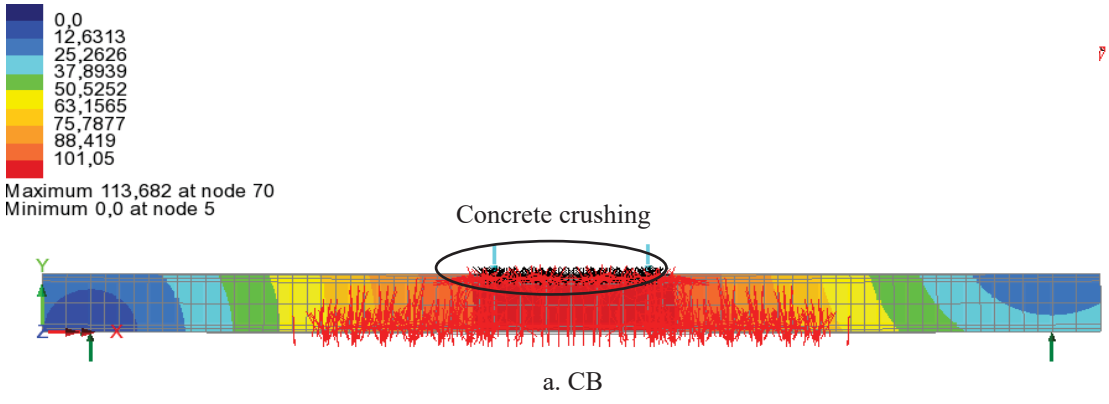

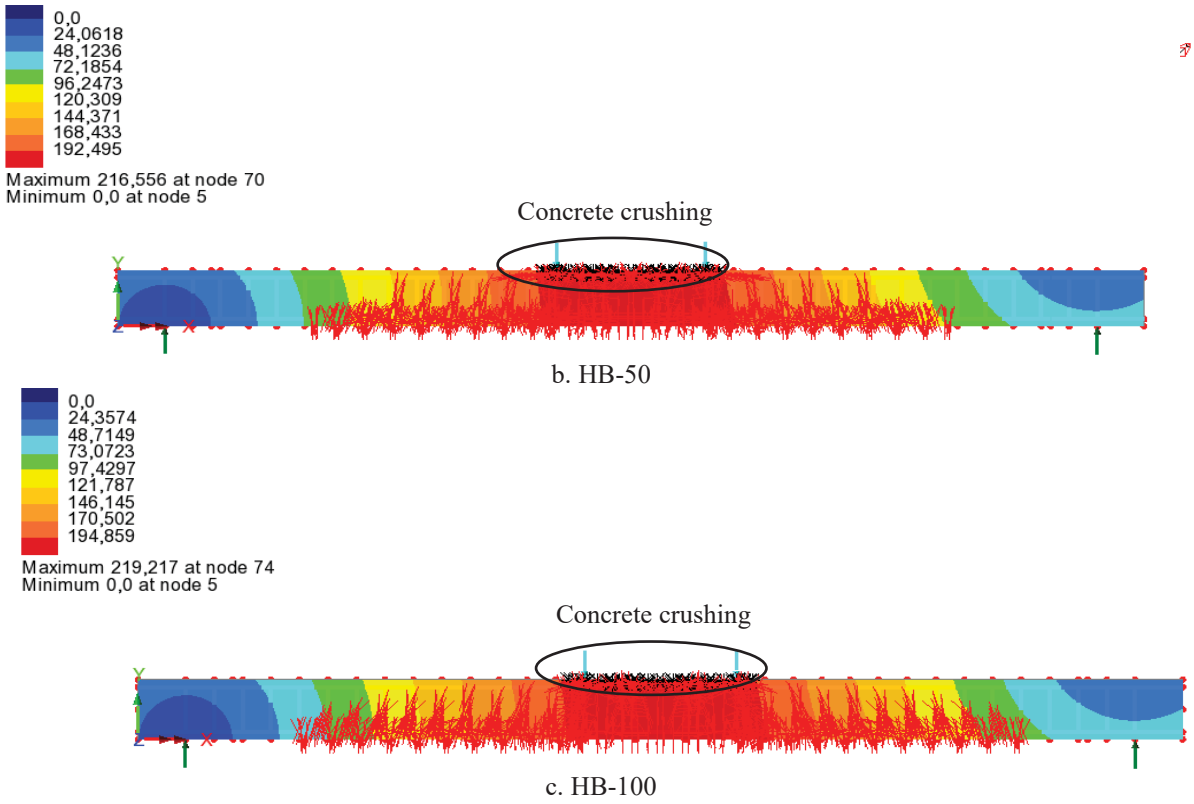

FIGURE 14. Crack pattern at the failure

CONCLUSIONS

The flexural performance of hybrid composite beams made of normal concrete and foamed concrete was conducted by using FEM Analysis, lead to the following conclusion:

1. The use of foamed concrete at hybrid composite beams reduced the ultimate load of the beams compared to the control beam, the ultimate load of HB-50 and HB-100 was decreased by 29.5% and 30.8%, respectively.
2. The different depths of foamed concrete at the hybrid beams had an insignificant effect on the ultimate load. The ultimate load of hybrid beam with 50 mm depth of foamed concrete was almost similar to 100 mm depth.
3. The number of cracks on HB-50 and HB-100 was larger than that of CB. This was because the foam concrete has a low tensile strength compared to normal concrete. In addition, some cracks in foam concrete do not propagate upward to the normal concrete layer. This was because there are interface in the foam concrete and normal concrete.

REFERENCES

1. P.M. Kumar and J.M.M. Paulo, *Concrete – Microstructure, Properties and Materials*, 3rd ed. (McGraw-Hill, 2005).
2. K.W. James and G.M. James, *Reinforced Concrete Mechanics and Design*, 6th ed. (Pearson, 2005).
3. S. Mindess, J.F. Young, and D. Darwin, *Concrete in Special Applications*, 2nd ed. (Pearson Education Inc., USA, 2003).
4. D. Rudy, B. Yasser, I. Rita, M.A. Abdul, and U.L. Rusdi, Int. J. Civil, Archit. Struct. Constr. Eng. **8**, 938–942 (2014).
5. A.A. Ahmmad, R.A. Sallal, J.A. Farid, A.A. Raad, and O. Mustafa, Structures **23**, 69–86 (2020).
6. G. Ballaji and R. Vetturayasudharsanan, Mater. Today Proc. **21**, 351–356 (2020).

7. Z. Wei, Q. Qinghua, L. Jianfeng, L. Kaikai, L. Poh, L. Yan, Z. Jianxun, X. Shejuan, C. Hongen, and Z. Jianping, Compos. Struct. **242**, 112175 (2020).
8. K.M.A. Hossaain, S. Hasib, and T. Manzur, Eng. Struct. **202**, 109856 (2020).
9. I. Rita, D. Rudy, B. Yasser, and M.A. Abdul, in *Conf. Civ. Eng. Res. Networks 2014* (Bandung, 2014).
10. A. Just and B. Middendorf, Mater. Charact. **60**, 741–748 (2009).
11. N.S. Syed, H.M. Kim, P.Y. Soon, Y. Jian, and C.L. Tung, Resour. Conserv. Recycl. **164**, 105103 (2020).
12. Y. Dingyi, L. Miao, and M. Zhiming, J. Build. Eng. **32**, 101509 (2020).
13. Y.H.M. Amran, N. Farzadnia, and A.A. Abang, Constr. Build. Mater **101**, 990–1005 (2015).
14. C. Bing, W. Zhen, and L. Ning, J. Mater. Civ. Eng. **24**, 113–11 (2012).
15. T.J. Chandni and K.B. Anand, J. Build. Eng. **19**, 154–160 (2018).
16. A.A. Hilal, N.H. Thom, and A.R. Dawson, Int. J. Eng. Technol. **7**, 286–293 (2015).
17. Readymix and Sonderdruck, *Fließfähiger Porenbeton,* (Transportbeton Beratungsgesellschaft, Ratingen, 1978).
18. ASTM C39/C39M, *Standard Test Method for Compressive Strength of Cylindrical Concrete Specimens* (American Society for Testing and Materials, West Conshohocken, PA, USA, 2003).
19. ASTM C78/78M, *Standard Test Method for Flexural Strength of Concrete (Using Simple Beam with Third-Point Loading)* (American Society for Testing and Materials, 2016).